Kuwait J.Sci., Vol.50, No.(1B),January.2023,pp(1-18)

Applications of well logging techniques to evaluate the groundwater aquifers in the area between southwest Bani Sweif and west Asyoute governorate, upper Egypt

Safi Eldein.M. Metwally [1], Shimaa. M. Elska [1,*], Fardous. M. Zarif [1], Abdallah. F. Saad [2]

[1] *Dept. of geophysical exploration, Desert Research Center, Cairo, Egypt*
[2] *Dept of Physics., Faculty of Science, Zagazig University, Zagazig, Egypt*

**Corresponding author: Shimaa_Elska@yahoo.com*

Abstract

The relevance of detecting aquifer characterization and aquifer potential has risen with the application of well logging technique as the demand for water has increased. Apart from pumping data, 16 geophysical well logs (resistivity, gamma ray, self-potential, and nuclear logs) are utilized to achieve the main goal of estimating petrophysical parameters (porosity ($\emptyset$), effective porosity ($\emptyset_{eff}$), hydraulic conductivity (k), permeability (K) and shale volume (V_{sh})) of the Apollonia (Eocene fractured limestone aquifer), Upper and Lower Bahariya (Nubian sandstone aquifer) formations. The findings show that the Eocene fractured limestone aquifer has a carbonate in soft chalk with high K and $\emptyset$ as well as high k of 4974.39 mD at well ST-188 (a highly productive aquifer), whereas the Lower Bahariya formation is mostly fine to medium-grained sandstone and clay, suggesting that it formed in shallow marine environments with low K. On the other hand, Upper Bahariya was noted that having poor sand succession. As results shown, K of the most examined wells range from 2609.69 to 1486.812 mD at ST-258 and ST-38 wells respectively. The study appears that V_{sh}, such as $\emptyset$ and K parameters, is regarded as an important attribute in aquifer evaluation where, estimated V_{sh} over the studied area is ranges between 5.96% and 31.7% at ST-48 and WBS1 wells respectively. Overall, this study provides an important insight into the importance of evaluating groundwater aquifers over time to help in making decisions to save and protect groundwater aquifers in the future for sustainable development.

Keywords: Bahariya formation; gamma; groundwater; neutron; Egypt

1. Introduction

Egypt is classed as a water-scarce country, despite its strategic location. It has a serious and long-standing water shortage, which might obstruct its economic growth (World Bank, 2018). The study area has been exposed to substantial deep groundwater extraction over the past three years as one of the new targeted reclamation areas. As a result, aquifer (s) appraisal as a dependable supply of water for agricultural and industrial sustainable development is urgently needed in such field region (Nisar *et al.*, 2021). Geophysical well logging is the most important method for determining subsurface petrophysical parameters, allowing researchers as Twfiq *et al*., (2021); and Zainab *et al*., (2019) to maximize field exploitation.

Little is known about the study area's aquifer, and its unclear what metrics are used to determine groundwater sustainability. Herein lies the significance of the current study, the primary purpose of which is to learn more about groundwater potential in various zones, as well as its lithological, petrophysical, and hydraulic properties. This was done by the examination and interpretation of all available geophysical well logs (nuclear logs, gamma ray, self-potential, and resistivity), as well as hydrogeological data. Consequently, evaluation of deep groundwater aquifers relates to the determination of aquifer properties such as porosity ($\emptyset$), effective porosity ($\emptyset_{eff}$), hydraulic conductivity (k), permeability (K) and shale volume (V_{sh}) (Farrag *et al.,*2019).

2. Study area and geological setting

The investigated area is located between Southwest Bani Sweif and West Asyoute in the western desert fringes of the North part of Upper Egypt (Figure 1).

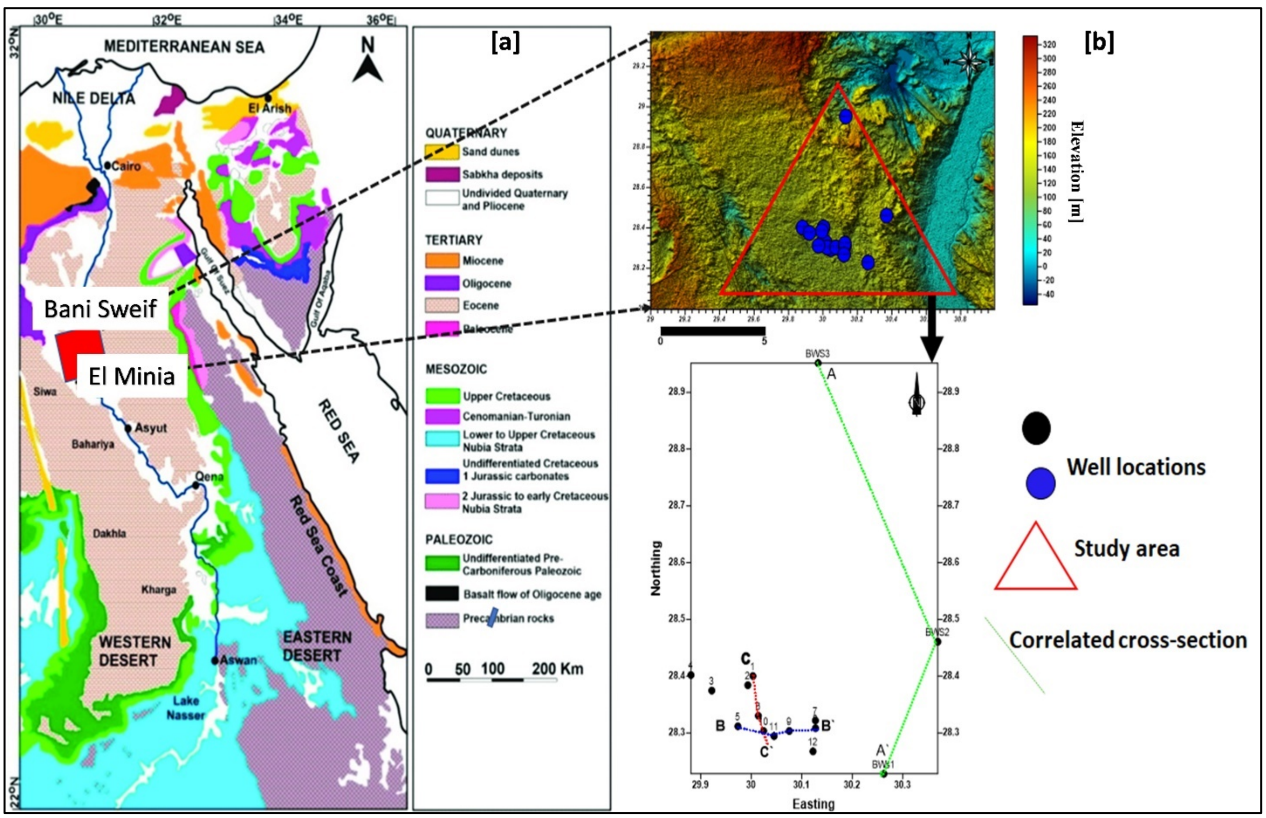

Fig.1. [a] a geological map with the location of study area modified after (Conoco,1987), [b]; a digital elevation map [DEM] of the study area with well locations

According to Yousif *et al*., (2018), the study area has four geomorphological units: tableland, floodplain (gravely, silt, and sandy plain), isolated hills, and a sand dunes belt (Figure 3). The Middle Eocene limestone aquifer, which is composed of the Samalut deposit (chalky limestone with thin clay intercalations), was identified as a water-bearing structure (Al-Ruwain, 1996). There were also several lithological units spanning in age from the Middle Eocene to the Quaternary (Figure 4). The study area is influenced by a network of faulting systems (NW-SE). These faults have a significant impact on the occurrences of groundwater aquifers in this region (Yousif *et al*., 2018). Figure (4) depicts a composite log tapped into West El Minia's shallow Bahariya aquifer in the Western Desert. The Bahariya Formation is classified into upper and lower units, and is mostly composed of fine to medium sandstone and clay (Wehr *et al*., 2002). The pre-Cambrian basement, a Cretaceous sequence that comprises the majority of the stratigraphic succession across the studied region, and the Apollonia formation, which is followed by Oligocene shales of the El Dabaa formation, make up the stratigraphy of the investigated area (Makky *et al*., 2014).

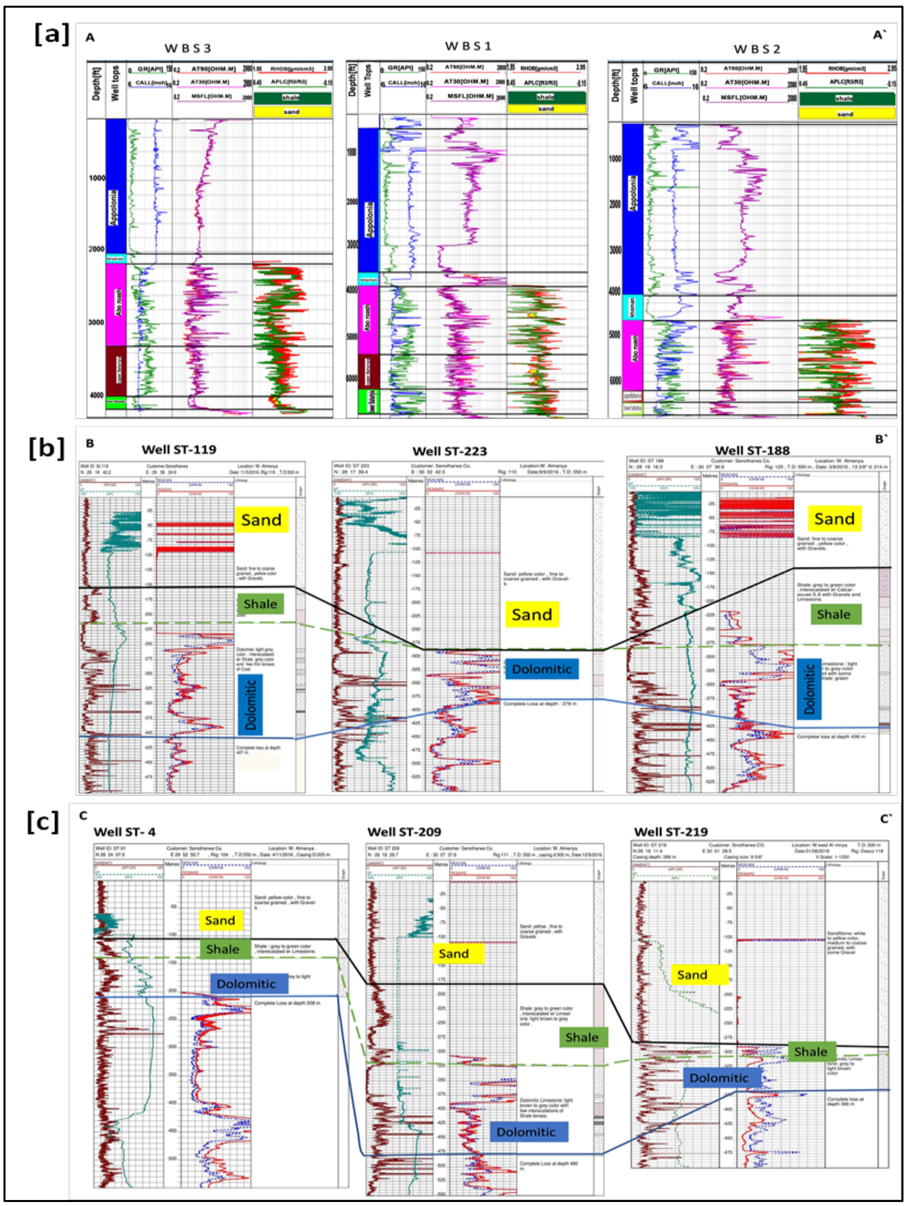

Fig. 2. Correlations among the tending well logs cross sections AA`, BB` and CC`

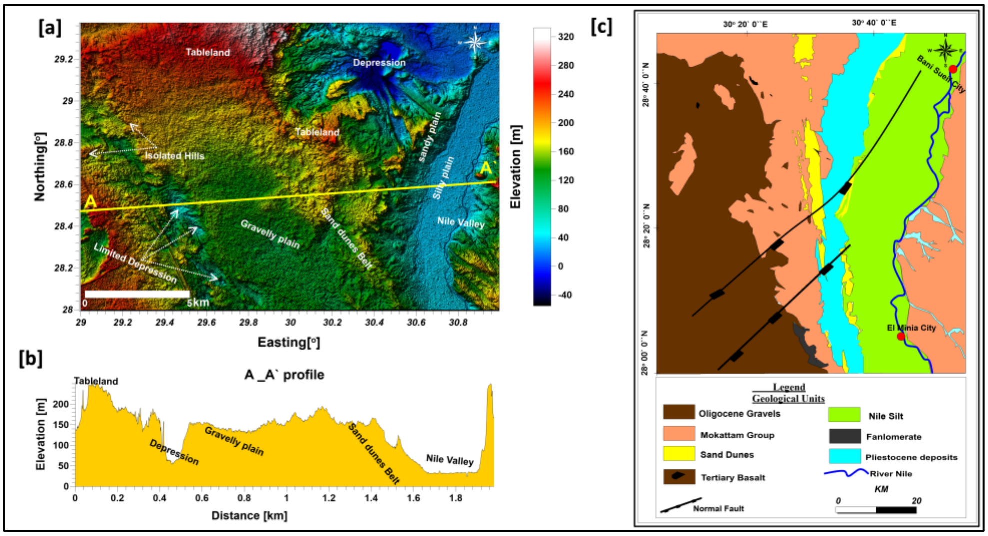

Fig. 3. (a) Geomorphology map of study area, (b) Geomorphic unit crossing study area along A-A` profile, (c) Geological unit of study area.

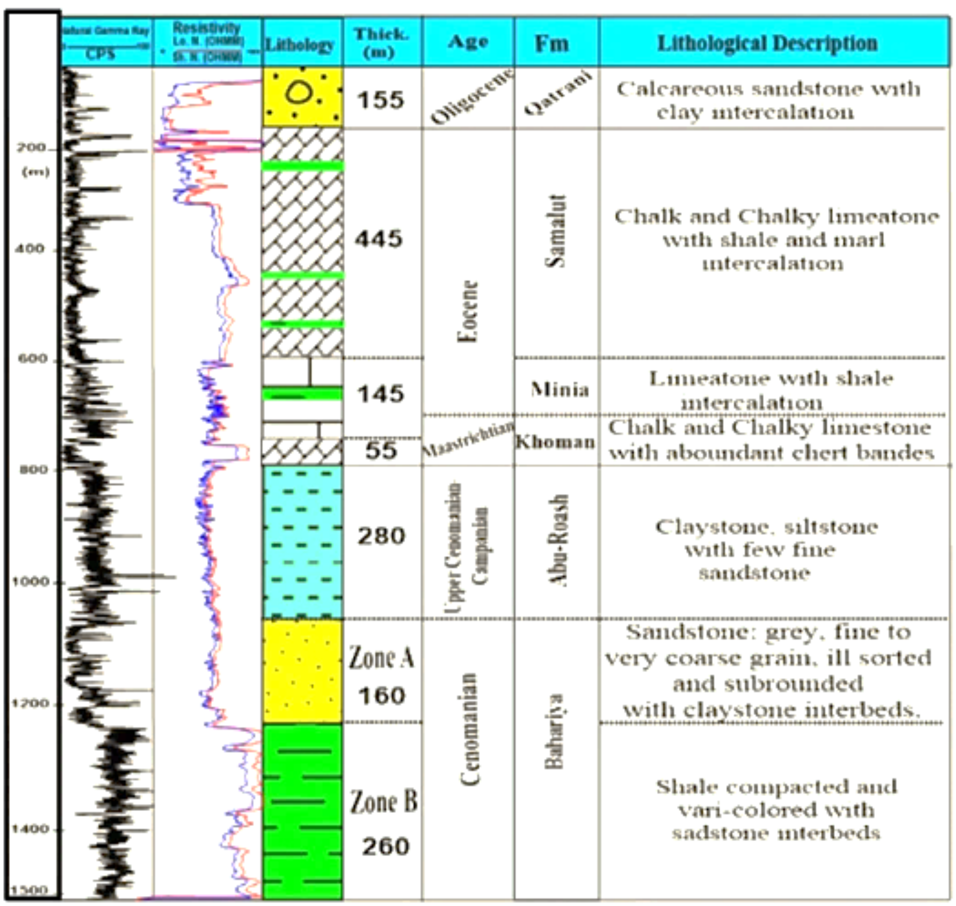

Fig. 4. Composite log tapping shallow Bahariya aquifer of west El Minia (Yousif *et al*., 2018)

3. Materials and methods

3.1 Data Acquisition

Sixteen Well logs were collected and depicted in Table (1). Some wells are correlated to demonstrate the subsurface stratigraphic strata (Figure 2) in the investigated area. The analysis of these well logs and 13 pumping test data were used to estimate the petrophysical and hydraulic parameters of the study aquifers.

Table 1. Available data for the study area

No	*name*	*Available data*
1	WBS 1	Density (RHOB), neutron (APLC), gamma ray (GR), resistivity (AT60-AT30-AT90), caliper (CAL), sonic (DT) logs
2	WBS 2	
3	WBS 3	
4	ST-13	GR, SP, long normal resistivity R46, short normal resistivity R16
5	ST -209	
6	ST-118	
7	ST-38	
8	ST-48	
9	ST119	
10	ST-180	
11	ST-188	
12	ST-214	
13	ST-223	
14	ST-258	
15	ST-1	
16	ST-219	

3.2. Data processing and interpretation

Well logs are collected in form of soft copies (Las files) and hard copies. To give a more realistic and accurate formation evaluation, the data of hard copies was digitized and stored in data files using the Golden Software Didger (V. 2.23) at depth intervals (0.5m in deep wells to 2m in shallow wells) and interactive petrophysics^{TM} (IP) software (http://www.senergyltd.com) was used to integrate all available data to understand and compute the input of the different petrophysical parameters. Self-potential, resistivity and gamma-ray logging curves were investigated in well logging data, with an emphasis on nuclear logs (density and neutron). The geophysical well logs are critical for determining the depth and thickness of viable zones as calculated aquifer characteristic (Shalaby, 2021; and Farrag *et al*.,2019).

3.2.1. Lithology identification

The lithology is determined from cross plots methods of the neutron-density, neutron-sonic, and M-N cross-plots.

3.2.2. Petrophysical parameters estimation

3.2.2.1. Shale volume

V_{sh} percentage is estimated from Gamma ray (GR) log by using equation of Schlumberger (1997):

$$V_{sh} = 0.5 * I_{GR}/(1.5 - I_{GR}) \quad (1)$$

$$I_{GR} = \frac{GR_{log} - GR_{min}}{GR_{max} - GR_{min}} \quad (2)$$

Where (I_{GR}) is gamma ray index, GR_{log} is the gamma ray log reading, GR_{min}, GR_{max} are the minimum and the maximum gamma ray reading.

The GR logs could discriminate between clean aquifer and poor one using shale base lines and identify the zone of water bearing. In these cases, the GR values in the water-bearing zones for studied well logs range from 120 American Petroleum Institute (API) in ST-119 well to150 API in WBS 3 well.

3.2.2.2. Porosity (∅): -

It can be calculated from neutron or density logs where ∅ equal to neutron logs reading or from density logs ($\emptyset_D$) by using the following equation of Asquith and Gibson (1982).

$$\emptyset_D = \frac{\rho_{ma} - \rho_b}{\rho_{ma} - \rho_f} \quad (3)$$

Where ρ_{ma} is matrix density, ρ_b is (bulk density) density log value, (ρ_f) is fluid density=1 g/cm^3 and from resistivity logs by using Archie´s formula (1942):

$$F = a^* \emptyset^m \quad (4)$$

Where, a is a constant =1; F formation factor= $R_t R_w$and m is a constant called cementation factor = 2 (empirically)

$$\emptyset = (1/(R_t/R_w)\ \hat{}1/2 \quad (5)$$

Where (R_t) is true resistivity in ohm m, and it obtained from comparing between long normal resistivity (R_{long}) and short normal resistivity (R_{short}) (Schlumberger ,1997)

$R_t = 1.7R_{long} - 0.7R_{short}$ (If R_{long}>R_{short}) (6)

and R_w is a formation water resistivity in ohm m which can be calculated from electrical resistivity (R) logs

$R_w = (R_{mf\times}R_t)/R_{short}$ (7)

Where, R_{mf} is mud filtrate resistivity and R_t is the true resistivity which was estimated from R_{long} and R_{short} curves.

3.2.2.3. Effective Porosity ($\emptyset_{eff}$):

It's calculated from the following equation (Schlumberger, 1997)

$\emptyset_{eff} = \emptyset * (1 - V_{sh})$ (8)

3.2.2.4. Hydraulic conductivity (*K*)

K calculates from $\emptyset_{eff}$ due to Schlumberger, (1997) by the following equation

$\emptyset_{eff} = 0.462 + 0.045 lnK$ (9)

3.2.2.5. The permeability (K)

K calculates from $\emptyset$ based on Timur (1968) formula:

K^1/2 $= 100 * \emptyset^{2.25} / S_{wirr} * 1000$ (10)

Where S_{wirr} is irreducible water saturation=5.2297 $\emptyset$

The water saturation (s_w) in the study area is~1. The depth to water (water bearing zone) can measure at specific depth based on R_t of induction log, SP, $\emptyset$ of density and neutron logs and Gamma ray log responses.

3.3. Pumping test

Firstly, the water level was monitored directly 2 hours before the pumping test was performed. The transmissivity will be estimated from specific capacity (Q/s) based on 13 pumping and recovery tests (Verbovsek, 2008).

T = C (Q/s). (11)

Where T is transmissivity m^2/day, Q/s is specific capacity m^3/day/m and C is constant at 0.9:1.5 value and an average of 1.2 (Jalludin and Razack, 2004). With the use of GWW software, T, *k*, and storage coefficient S were calculated using the Theis method (1935).

4. Results and discussion

The petrophysical properties of the Nubian sandstone aquifer were elucidated by the well-logging study. A variety of cross plots were created and interpreted. The Eocene carbonate aquifer was assessed using the standard archie (1942) and schlumberger (1997) equations.

4.1. Apollonia formation Evaluation

Due to the shortage of neutron, sonic, and density log recordings. The following contour maps will be depended mainly on the above equations. Figure (5a) shows the distribution of depth to Apollonia waterbearing that increases in south and south east direction. Figure (5b) depicts the water level contour map which displays that water level values range from 8m to - 259m. The water flow direction is towards the southwest direction where the recharge source is the Nile valley where, Figure (5c) represents the distribution of porosity ($\emptyset$) which increases in the south and southeast of the study area, reaching a maximum of 46.96 % at ST-258 well and a minimum of 18.31 % at ST-38 well. Estimated effective porosity ($\emptyset_{eff}$) over the study area is shown in (Figure 5d), which shows the similar trend of ($\emptyset$). Table (2) summarized the estimated petrophysical parameters for Eocene carbonate aquifer. The permeability contour map is depicted in Figure (5e). It increases in the south and east directions, where it has a high value of 2609.69 mD at ST-258 well, and decreases in the southwest direction, where the minimum value is 1486.81 mD at ST-38 well. The hydraulic conductivity contour map (Figure.5f) has the same trend of permeability distribution. Iso resistivity contour map is shown in Figure (5g). The resistivity values are increase in west and northwest direction with maximum value 138. 89 Ohm.m at well ST-19. The results show also the distribution of V_{sh} Figure (5h) which increases towards east and northeast direction (Nile valley direction). The low V_{sh}% meaning that Apollonia formation is mainly carbonate rocks with little intercalation of shale.

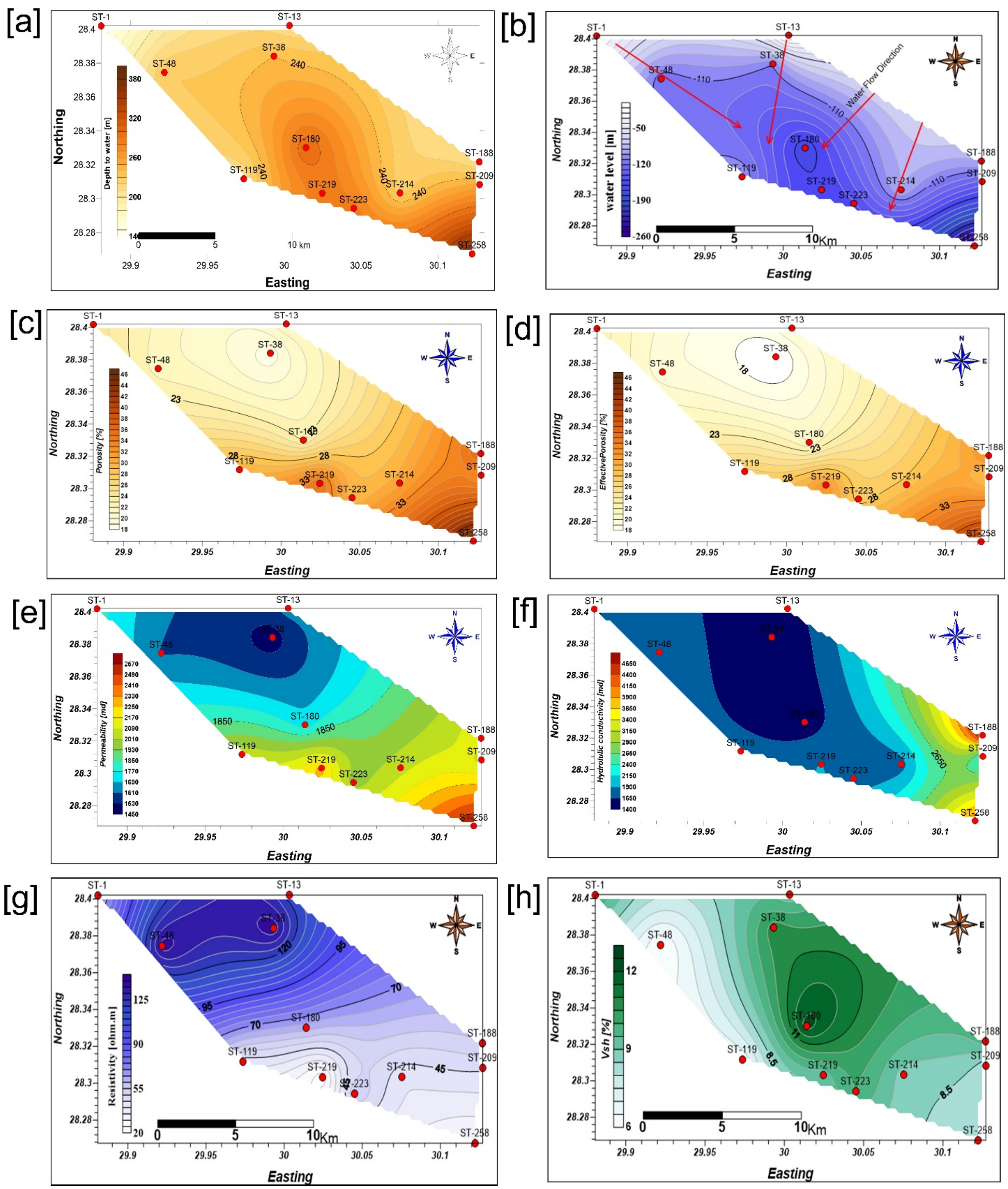

Fig. 5. [a] depth to water. [b] water level. [c] porosity, [d] effective porosity, [e] permeability [f] hydraulic conductivity, [g] Isoresistivty and [h] shale volume percentage contour maps for Apollonia formation.

The estimated V_{sh} of the studied wells (Figures. 6a & b) demonstrate that Apollonia and Upper Bahariya formations are classified as clean aquifers have low shale content. The Apollonia Formation's shale volume was shown in Figure (6a). It reveals that the formation has the least amount of shale, followed by the upper and lower Bahariya formations in decreasing depth order (Figure.6b). The average V_{sh} values for the three formations are 8%, 20%, and 26 %, respectively.

Table 2. Summarized petrophysical parameters of geophysical well logs:

Well	Aquifer	Coordinate N	E	Total thickness(m)	Total depth (m)	Depth to water(m)	water level(m)	Ø (%)	Ø$_{eff}$(%)	k (mD)	k (mD)	V_{sh}(%)
WBS1	UPPER	30.2623	28.2279	99.3648	2072.64	1644.0912	*	21.721	14.9232	1695.4956	1348.8905	31.5812
WBS2	BAHARIYA	30.3690	28.4607	82.6008	2103.12	1892.5032	*	17.903601	17.7547	3087.6849	1523.8235	14.7649
WBS3		30.1324	28.9517	214.2744	1310.64	1009.1928	*	27.9716	18.1721	1878.5813	1345.0364	31.0552
WBS1	LOWER	30.2623	28.2279	302.3616	2072.64	1743.456	*	24.536	13.2508	1585.3528	1310.1223	32.0335
WBS2	BAHARIYA	30.3690	28.4607	86.8395	2103.12	1975.104	*	19.39167	17.5610	1964.3312	1440.1947	26.0592
WBS3		30.1324	28.9517	53.0352	1310.64	1223.4672	*	24.7386	18.0292	1750.9523	1460.8821	22.9095
WBS1	APOLLONIA	30.2623	28.2279	963	2072.64	102	37.68	*	*	*	*	5.0433
WBS2		30.3690	28.4607	1189	2103.12	129	44	*	*	*	*	4.9527
WBS3		30.1324	28.9517	618	1310.64	108.32	38.28	*	*	*	*	12.0628
ST13		30.0033	28.4022	365	580	98.95	33.05	22.04855	20.3482	1647.970	1528.0260	9.1357
ST38		29.9932	28.3841	305	550	96.74	34.26	18.30979	16.5387	1486.817	1397.3693	10.7701
ST48		29.9219	28.3745	280	540	80.48	32.52	21.50817	19.3537	1604.814	1902.4103	5.9646
ST1		29.8807	28.4019	348	550	91.9	35.1	24.79189	22.7151	1804.375	1622.8801	10.1588
ST119		29.9736	28.3117	270	500	76.9	33.1	30.02235	27.3983	2064.033	1737.3048	6.5722
ST180		30.0141	28.3301	170	500	97.4	33.6	22.80661	20.9547	1725.351	1521.9702	12.264
ST188		30.1269	28.3217	325.5	550	85.4	34.6	36.74754	33.0401	2165.998	4974.3917	9.7705
ST209		30.1271	28.3083	245	550	85.21	35.79	32.60873	27.9922	2060.183	2254.0058	8.1773
ST214		30.0753	28.3034	275.5	500	99.69	36.31	30.6382	28.4832	2064.033	1785.2611	8.7479
ST219		30.0246	28.3032	210	530	88.15	36.85	35.50314	32.0514	2275.824	1912.2649	9.2288
ST223		30.0451	28.2943	325	550	97.2	35.8	29.03656	27.3328	1970.151	1784.8808	10.0485
ST258		30.1222	28.2674	233.172	700	83.25	37.75	46.96442	42.56449	2609.695	4171.2785	8.4168

* No data, mdarcy (mD), Porosity (Ø), Effective Porosity (Øeff), permeability(k), hydraulic conductivity(k), Shale Volume $\boldsymbol{V_{sh}}$

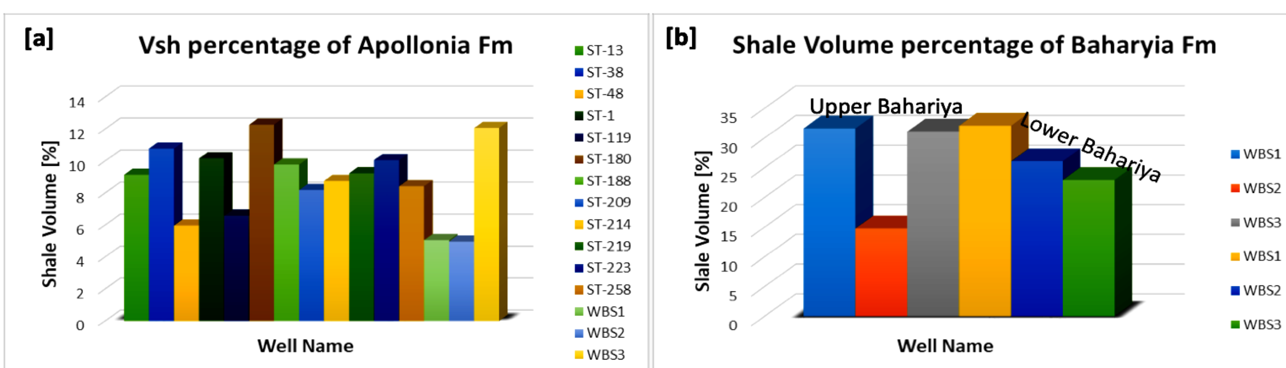

Fig. 6. Clustered column for [a] percentage of shale volume of Apollonia Fm of available wells, [b] the percentage of shale volume of upper and lower Bahariya Fm for three deep wells.

4.2. Bahariya formation evaluation

The Nubian sandstone aquifer was evaluated using the derived petrophysical characteristics. Figure (7) illustrates the findings of the neutron density cross plot, which demonstrates how groundwater affects the plotted data as it migrates northwestern from the limestone line. A drop in the phi neutron ($\emptyset_N$) and a rise in the phi density ($\emptyset_D$) are both signs of this phenomenon. The highest ($\emptyset_D$) for the upper Bahariya formation is 0.45 at well WBS1 (Figure.7a) and the lowest is 0.0038 at well WBS3 (Figure.7c). At well WBS1 (Figure.7a), the highest ($\emptyset_N$) is 0.451, while the minimum is 0.093 (Figure.7b). Due to the movement of displayed data toward the southwest of the cross plot, the shale impact in WBS3 is higher than in WBS1 and WBS2.

The lower Bahariya formation's highest ($\emptyset_D$) is 0.4478 at well WBS1 (Figure.7a), while the lowest ($\emptyset_D$) is 0.000645 at well WBS2 (Figure.7b). In addition, the highest ($\emptyset_N$) for the lower Bahariya formation is 0.447 at well WBS1 (Figure.7a), while the minimum ($\emptyset_N$) is 0.067 at well WBS2 (Figure.7b). It was discovered that shale affects WBS2 more than WBS1 and WBS3 wells.

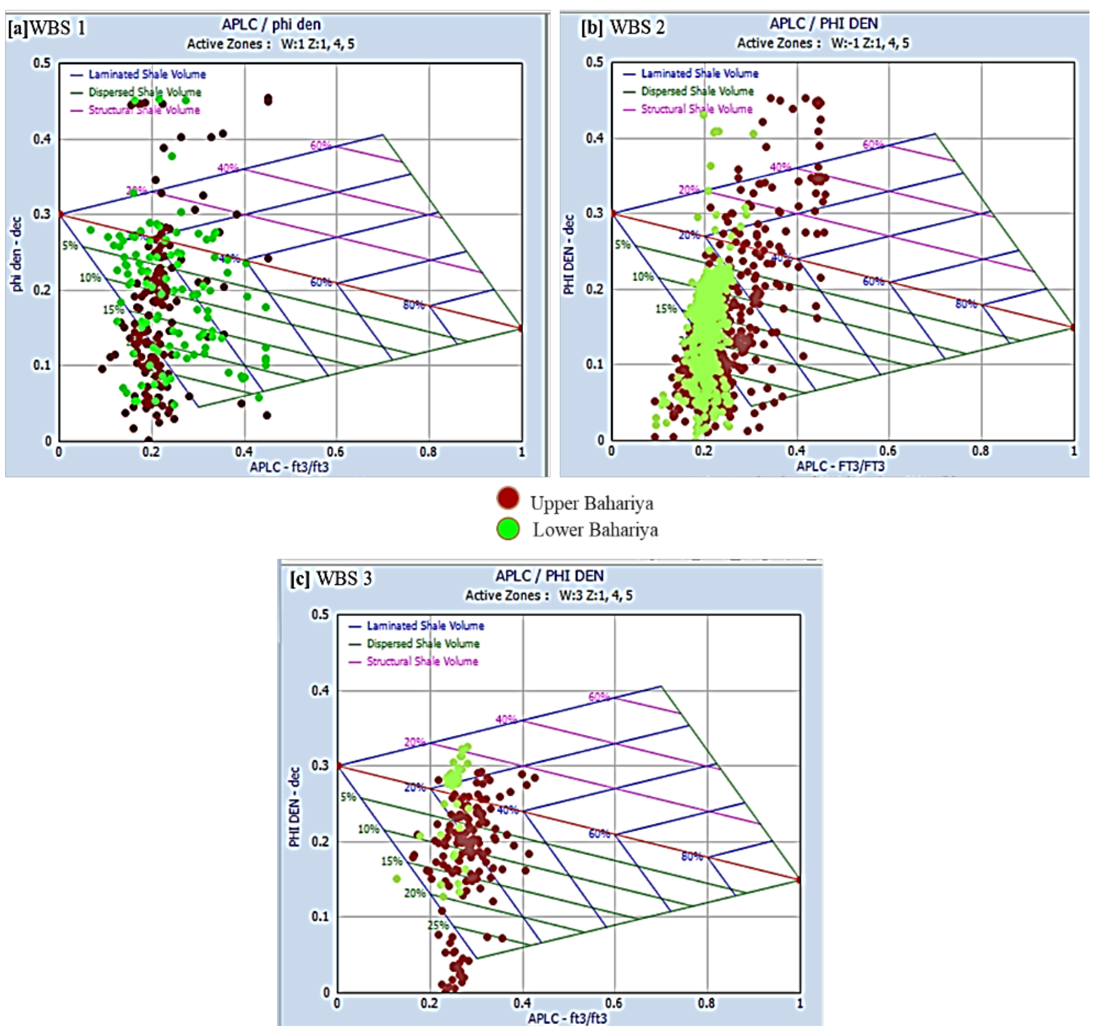

Fig. 7. Shale type cross plot of upper and lower Bahariya formation; [a] WBS 1, [b]; WBS 2 and [c]; WBS 3 wells.

Figure (8) depicts the relationship between GR and $\emptyset_N$ in terms of energy (APLC). This cross plot shows that the presence of limestone and dolomite is indicated by low GR and low (APLC) points. Sandstone rock units are indicated by medium GR and medium APLC points, whereas shale is indicated by high GR and high APLC points. The WBS1 at figure (8a) exhibits a moderate GR and APLC for the upper and lower Bahariya formations, indicating that the lithology of this formation is mostly sandstone.

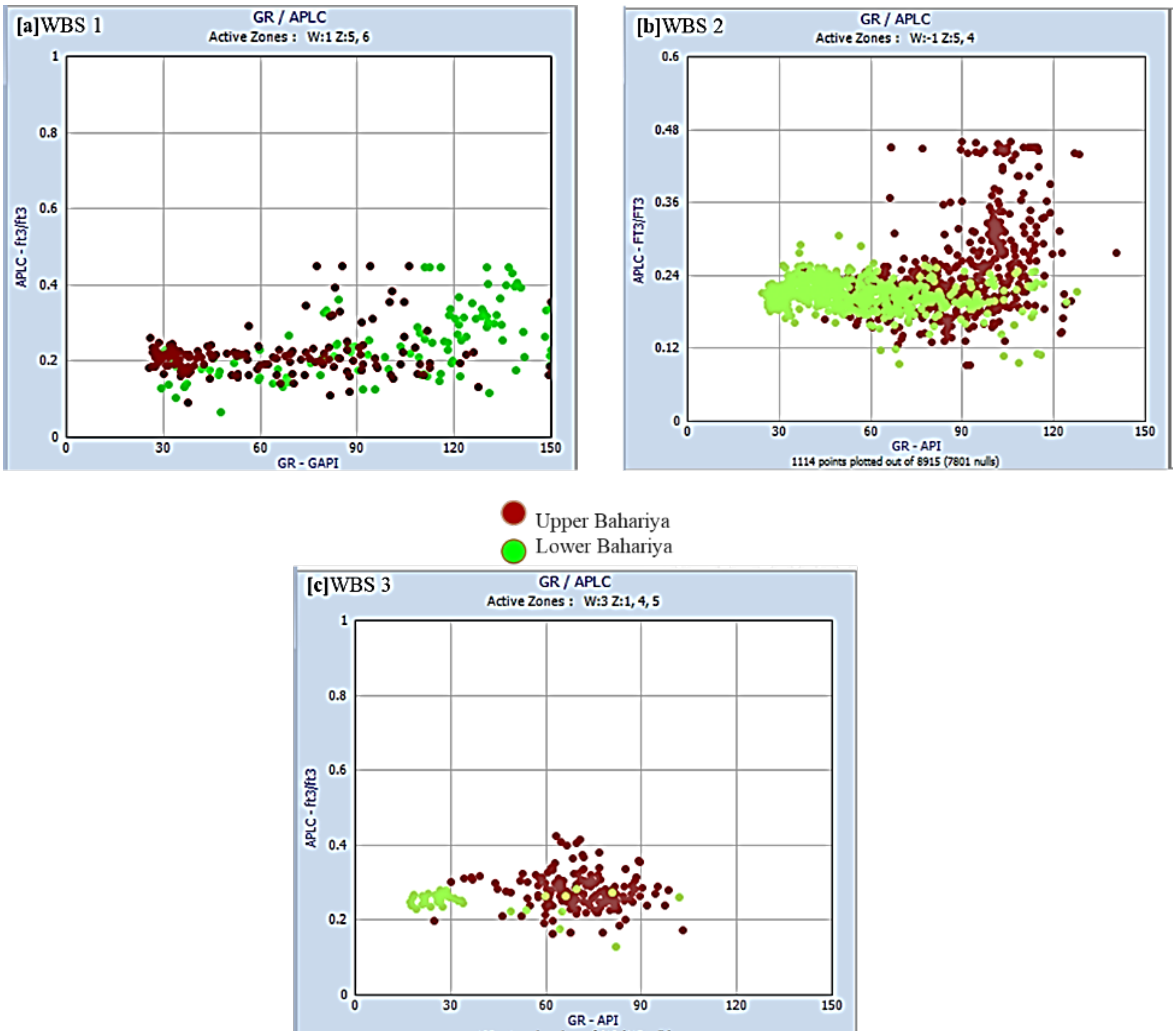

Fig. 8. GR- APLC cross plot [a]; WBS 1 [b]; WBS 2 and [c]; WBS3 wells.

Figure (9) clarifies the results of the GR and density logs (RHOB), where plots reveal that points of limestone and dolomite are displayed in the left direction. As a result, the major lithology of this aquifer may be concluded to be sandstone with shale and carbonate streaks based on plotted sites along the sandstone line are the highest.

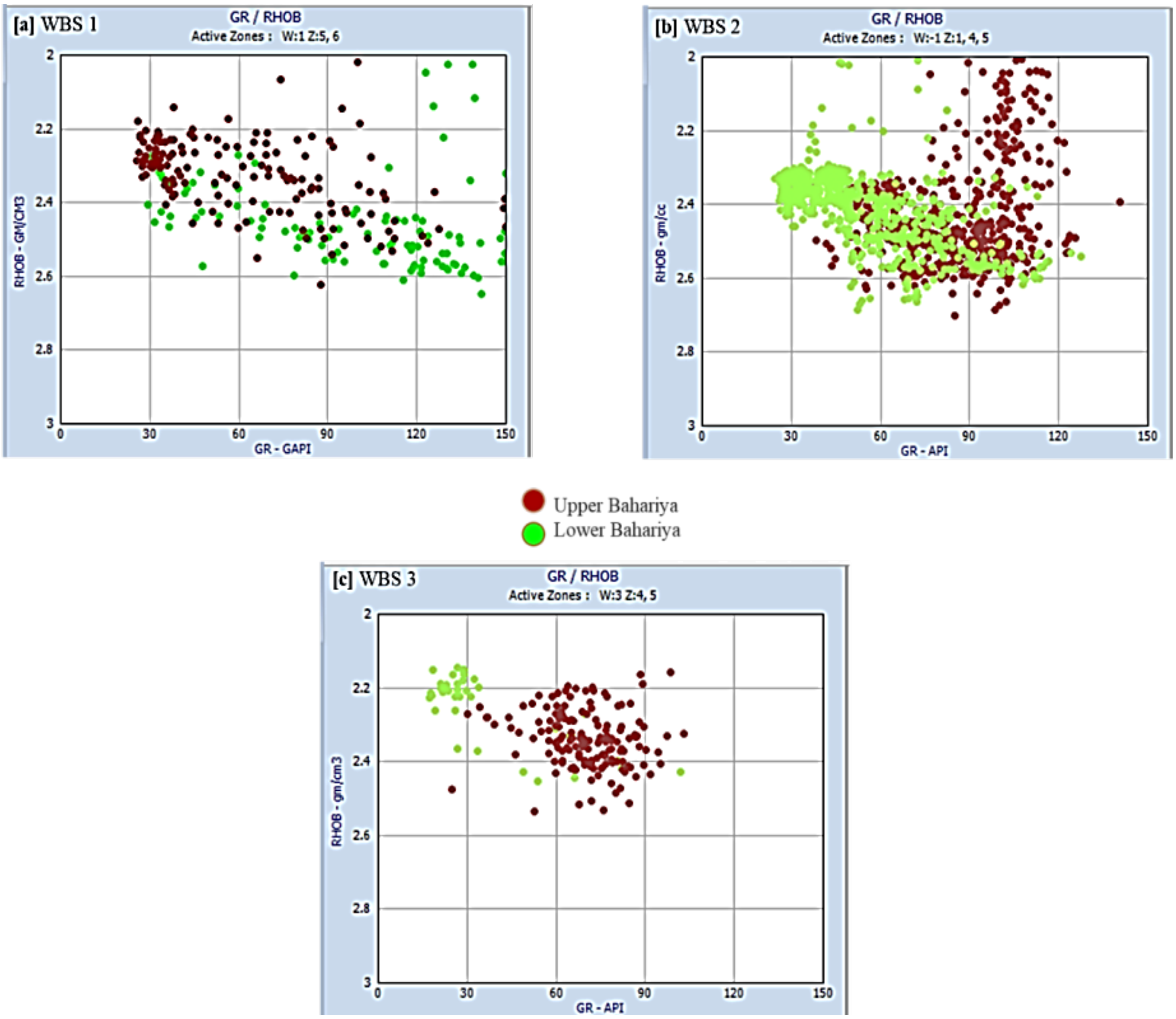

Fig. 9. GR-RHOB cross plot [a]; WBS 1 [b]; WBS 2 and [c]; WBS3 wells

Figure (10) shows a cross plot of porosity and lithology for the upper and lower Bahariya formations. Figure (10a) shows plotted data from the upper Bahariya well at WBS1, which is dispersed between sandstone and limestone and has a porosity value varying from 9.3 to 46.1%. The bulk of points appear to be spread downward along the dolomite line due to the impacts of shale. This indicates the presence of shale lithology in sandstone and limestone lines. The data from the lower Bahariya aquifer's neutron–density cross plot is distributed between the sandstone line and limestone, with porosity values ranging from 6.7 to 44.7 %. The upper Bahariya formation is therefore cleaner than the lower Bahariya formation. These findings match with those of Ghoubachi (2017) and Yousif *et al.* (2018), who found that the Bahariya formation is separated into two units as documented in well logs, and that their productivity is mostly determined by the proportion of (V_{sh}).

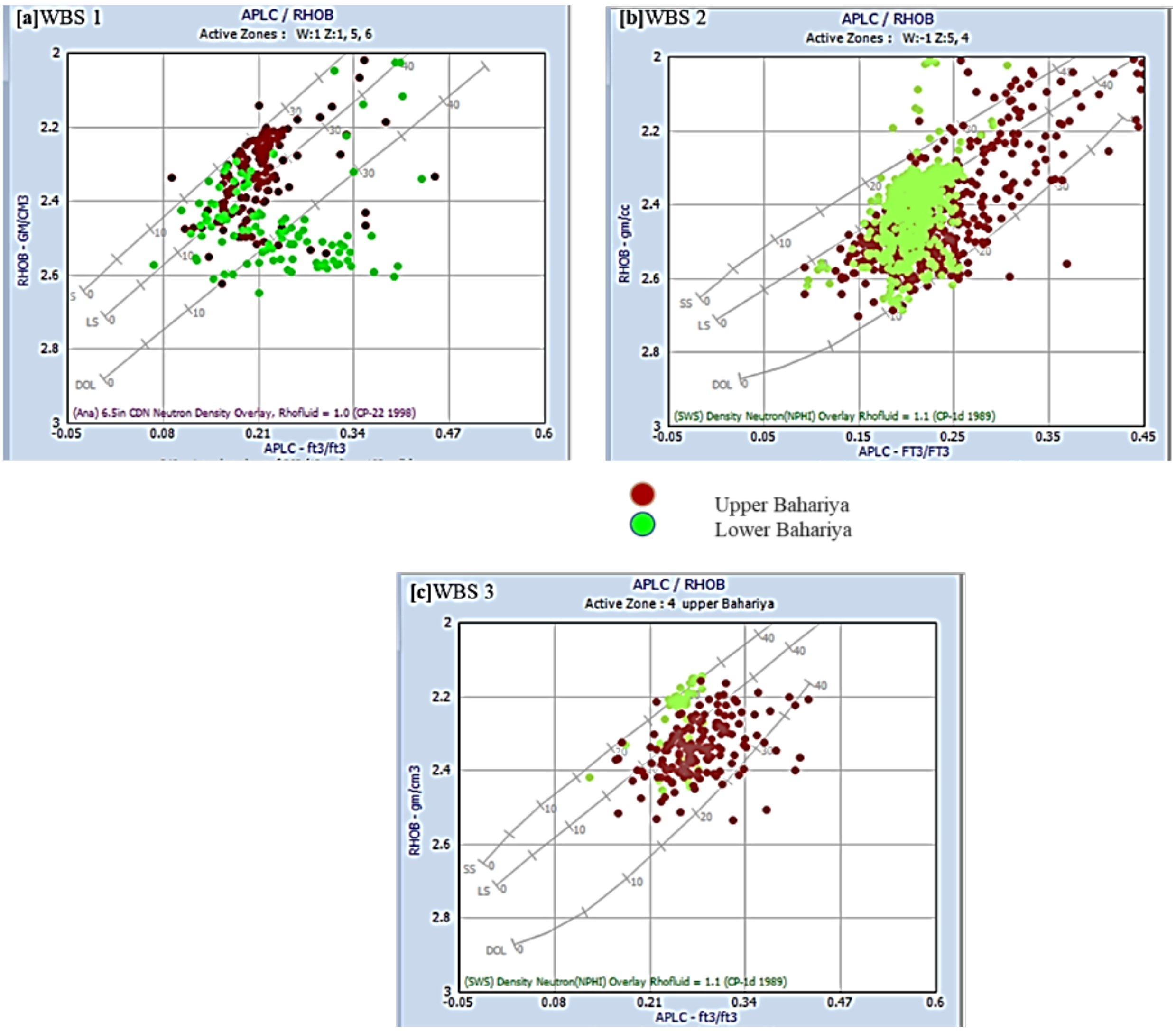

Fig. 10. APLC/RHOB cross-plots of Bahariya formation for [a] WBS 1, [b] WBS 2 and [c] WBS 3 wells

5. Hydrology

Table (3) shows the results of the preliminary analysis of pumping tests using equation (11) for unconfined Eocene aquifer. The quick time recovery (29:120 min), (Figure. 11), is most likely due to the secondary porosity of the fissured limestone aquifer. This aquifer is distinguished by two types of water flow (laminar and turbulent flows) (Ibrahim *et al*., 2020). *K*, T, and S were calculated using long-duration pumping test of 13 wells. According to the fitted models of these wells, the tested *K* values range from 0.25×10^1 to 4.15×10^1 m/d with an average of 2.1×10^1 m/d (Table 3). The wide range of *K* values can be explained by permeable zones caused by the karstification process, which is accompanied with fast changes in the high density of fractures and joints as observed in wells ST38, 214, and 48 (Figure. 11).

Table 3. Finding of pumping test analysis of Eocene fractured limestone aquifer.

WELL NO.	AQUIFER	FORMATION	PUMPING RATE Q (M^3/H)	DRAWDOWN S (M)	SPECIFIC CAPACITY ($M^3/H/M$)	LOSS FACTOR B (M)	T (M^2/DAY)	SALINITY (MG/L)	K (M/D)	SAFE YIELD	WELL PRODUCTIVITY CLASSIFICATION (IBRAHIM, 2020)
ST1	Eocene	Apollonia	215	3.5	61.43	345	9400	2304	2.75×10^0	150	High
ST13			220	2.7	81.5	0	229	2384	2.65×10^0	150	High
ST38			215	7.20	29.86	200	937	2320	0.25×10^3	150	High
ST48			210	1.39	151.079	200	8300	2194	4.15×10^1	150	High
ST119			220	21.18	10.387	280	348	2048	4.57×10^0	150	High
ST180			210	10.85	19.35	202	2540	2285	1.46×10^1	150	High
ST188			210	13.22	15.885	337	2240	2208	7.27×10^0	150	High
ST209			200	6.98	28.65	250	3140	2426	1.27×10^1	150	High
ST214			200	10.06	18.87	275	2990	2304	1.10×10^1	150	High
ST219			240	12.15	19.75	241	1790	2340	8.30×10^0	150	High
ST223			190	13.90	13.669	267	1140	2342	4.87×10^0	150	High
ST258			180	42.71	4.21	358	598	2451	1.68×10^0	150	High

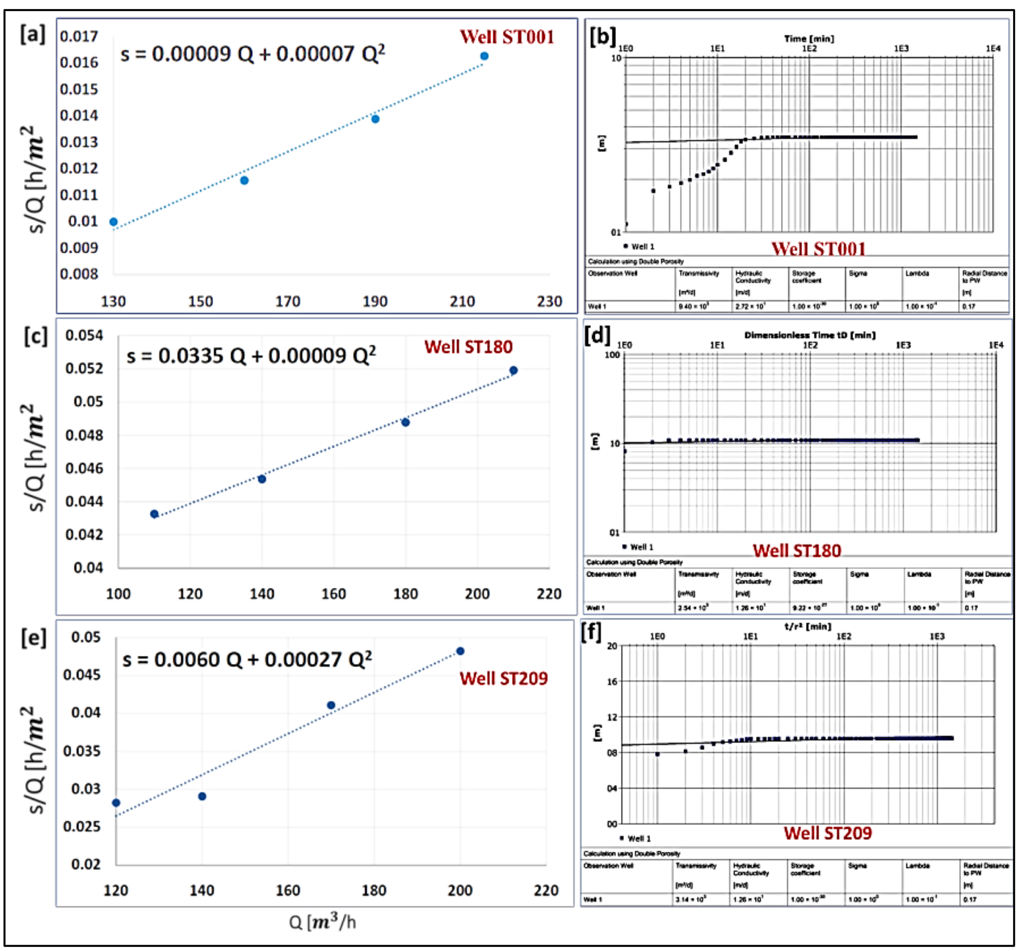

Fig.11. Long-duration tests data analysis for some Eocene aquifer over the investigated area. a, c and d represent the relationship between the rate of withdrawal and qualitative decline, while b, d and f represent the results of the analysis of long pumping test using the Theis method.

6. Conclusion

The available geophysical well logging data and pumping tests were complementary each other to obtain the detailed hydrogeological characteristics of the Eocene and Nubian sandstone aquifers in the study area. The lower Bahariya unit has the lowest hydraulic characteristics and the most modest petrophysical qualities. For any future well drilling/production activity, the study strongly recommends extracting from the Upper Bahariya unit of the Nubian sandstone aquifer of low V_{sh} with a priority of WBS2 well, whereas in the Eocene aquifer, the total extraction rate per day should not exceed 150 m^3/day in the entire study area to prevent depletion of the concerned aquifer. As a result, the implied geophysical well logging technique and its accompanying detailed petrophysical analysis contributed to a better understanding of the characteristics of the Eocene and Nubian sandstone aquifers in this specific area of Egypt's western Desert, where many complex geological and hydrogeological aspects occur. Furthermore, the current study indicated that $\emptyset_{eff}$, k, and V_{sh} are the primary determinants of Eocene and Nubian sandstone aquifers quality, all of which are critical in optimizing sustainable groundwater resource management techniques.

References

Archie, G. E., (1942). The electrical resistivity log as an aid in determining some reservoir characteristics. Trans., AIME, 146, 54-67.

Asquith, G. & Gibson, C. (1982). Basic Well Log Analysis for Geologists. AAPG Publications, Tulsa, OK, 216 pp.

F.M. Al-Ruwain. (1996) Hydrogeology and ground water modeling of the carbonate aquifer of Al-Sulibiya, Kuwait. Kuwait J.Sci. &Eng.23, 1996.

Farrag, A. A., Ebraheem, M. O., Sawires, R., Ibrahim, H. A., & Khalil, A. L. (2019). Petrophysical and aquifer parameters estimation using geophysical well logging and hydrogeological data, Wadi El-Assiuoti, Eastern Desert, Egypt. Journal of African Earth Sciences, 149, 42–54. https://doi.org/10.1016/j.jafrearsci.2018.07.023

Ghoubachi, S.Y., (2017). The hydrogeological characteristics of the Nubian Sandstone System in Sahl Karawein Area and Its Vicinities, El-Farafra Oasis, Western Desert, Egypt. Ann. Geol. Surv. Egypt. 36, 175–187.

Ibrahem, S. M. M., Elalfy, M., Hagras, M. A., & Company, A. (2020). Groundwater Potentials of Eocene, 82(1), 59–82.

Jalludin, M., and Razack, M., (2004): Assessment of hydraulic properties of sedimentary and volcanic aquifer systems under arid conditions in the Republic of Djibouti (Horn of Africa),Hydrogeol. J.,12(2), 159-170.

Makky, A. F., El Sayed, M. I., Abu El-Ata, A. S., Abd El-Gaied, I. M., Abdel-Fattah, M. I., & Abd-Allah, Z. M. (2014). Source rock evaluation of some upper and lower Cretaceous sequences, West Beni Suef Concession, Western Desert, Egypt. Egyptian Journal of Petroleum, 23(1), 135–149. https://doi.org/10.1016/j.ejpe.2014.02.016

Twfiq Mohamed Z., Zarif Fardous. M., Massoud A. and Al Temamy Ayman M., (2021). Determination of the petrophysical and natural radioactivity properties of Nubian sandstone Aquifer at the area of the Northwest El Ain village, Sharq El Oweinat area, southwestern Desert, Egypt. Asian journal of Environment &Ecology.15(4):37 55,2021. Doi:10.9734/AJEE/2021/v15i430236.

Nisar, U. B., Khan, M. J., Imran, M., Khan, M. R., Farooq, M., Ehsan, S. A., Ahmad, A., Qazi, H. H., Rashid, N., & Manzoor, T. (2021). Groundwater investigations in the Hattar industrial estate and its vicinity, Haripur district, Pakistan: An integrated approach. Kuwait Journal of Science, 48(1), 51–61. https://doi.org/10.48129/KJS.V48I1.7820.

Schlumberger (1997), L Interpretation, Principles/Applications. Houston, Texas, U.S.A.

Shalaby, M. R. (2021). Petrophysical characteristics and hydraulic flow units of reservoir rocks: Case study from the Khatatba Formation, Qasr field, North Western Desert, Egypt. Journal of Petroleum Science and Engineering, 198, 108143. https://doi.org/10.1016/j.petrol.2020.108143.

Theis, V., (1935). The relation between the lowering of the piezometric surface and the rate and duration of discharge of a well using groundwater storage. Transaction of the American Geophysical Union. 16:519-524.https://doi org/10.1/29623

Timur, A. (1968): An investigation of permeability, porosity, and residual water saturation relationships. Log Anal. 9(4), 8–17.

Verbovsek, T., (2008): Estimation of transmissivity and hydraulic conductivity from specific capacity and specific capacity index in Dolomite aquifers. J. Hydrologic Eng., 13(9).

Wehr, F., Youle, J. and Pemberton, G. (2002). Sequence stratigraphy and sedimentology of the Bahariya Formation, Khalda Concession, Western Desert, Egypt. American Association of Petroleum Geologists, International meeting, Cairo, Egypt, (Abstract Volume unpaginated).

World Bank. (2018). Water scarce Cities: Thriving in a finite world.

Yousif, Mohamed, Hassan S. Sabet, Saad Y. Ghoubachi, and Ameer Aziz (2018). "Utilizing the Geological Data and Remote Sensing Applications for Investigation of Groundwater Occurrences, West El Minia, Western Desert of Egypt." NRIAG Journal of Astronomy and Geophysics 7(2):318–33.

Zainab, M. H. A. L., Almallah, I. A., & Al-Najm, F. M. (2019). Petrophysical properties evaluation using well logging of the upper sand member of Zubair Formation in Zubair oil Field, Southern Iraq. Basrah Journal of Science, 37(3), 457–480.

Submitted: 21/11/2021
Revised: 21/02/2022
Accepted: 09/03/2022
DOI: 10.48129/kjs.17333